Experimental Prediction of Nonlinear Dynamics and Reconstruction of Statistical Properties via Reservoir Computing (ESN)

Yuxiu Guo
School of Physics and Astronomy, Class of 2023

Abstract

In this work, we study an experimental time series collected from a simplified RLC magnetic rotor apparatus with a common-mode inductor. We employ an Echo State Network (ESN; Reservoir Computing) to reconstruct the underlying system dynamics, perform short-term trajectory (orbit) prediction, and evaluate the agreement between the model and measurements in terms of selected statistical quantities (autocorrelation and power spectrum) as well as predictability scales (the maximal Lyapunov exponent). We compared two prediction settings: **open-loop** (with an external driving signal as input) and **closed-loop** (autonomous evolution where previous predictions are fed back as the next-step input). Our results show that ESNs achieve highly accurate short-term pointwise prediction under open-loop driving, whereas under fully closed-loop operation the pointwise error grows over time. We further discuss the reproducibility of the maximal Lyapunov exponent estimated from closed-loop predictions: if a naive fit of the logarithm of the true–prediction error yields a negative value, this typically reflects issues in methodology/window selection or model dissipation rather than the system being "truly stable." Finally, we outline possible future directions and discuss potential reasons for the failure of low-rank RNNs in this task, together with suggestions for improvement.

Keywords: Echo State Network (ESN); reservoir computing; closed-loop prediction; Lyapunov exponent

1. Introduction

In recent years, machine learning methods have rapidly advanced in applications to nonlinear dynamical systems. In particular, the success of Echo State Networks / reservoir computing in noisy time-series prediction and dynamical reconstruction makes it possible to infer short-term trajectory behavior and long-term statistical "climate" directly from observational data. In this study, we investigate a periodically driven magnetic rotor device containing nonlinear elements, model its time series using an ESN, and compare two prediction modes: **open-loop** (driven) and **closed-loop** (autonomous evolution). Our goals are: (i) to validate the ESN's capability for short-term trajectory prediction, and (ii) to establish a robust workflow for estimating the maximal Lyapunov exponent.

2. Theory and Methods (Overview)

2.1 Echo State Network (ESN)

An ESN models time series using a large recurrent network (the **reservoir**) with randomly fixed weights, together with a linear readout layer trained via ridge regression. Because training reduces to solving a linear regression problem, ESNs are computationally efficient and relatively easy to tune. Key components used in this work include:

Input vector: $u(t) = [\sin(\theta(t)), \cos(\theta(t)), u_{\text{drive}}(t)]$.

- **Output:** $y(t) = \theta(t)$(in radians; with 2πwrapping handled in post-processing).
- **Training:** ridge regression to solve the output weights W_{out}.
- **Key hyperparameters:** reservoir size (res_dim), spectral radius, leaking rate, sparsity, ridge regularization.

2.2 Angular Error Metric

To avoid error distortion caused by 2πdiscontinuities, the angular error is defined using a wrapped difference:

$$\Delta\theta = \text{mod}(\hat{y} - y + \pi, 2\pi) - \pi.$$

We report MAE, RMSE, and normalized RMSE (e.g., RMSE/2π or RMSE/std) as evaluation metrics.

2.3 Estimating the Maximal Lyapunov Exponent (Method Summary)

We estimate the maximal Lyapunov exponent λ_{max}using a **two-trajectory divergence** approach: we evolve two closed-loop trajectories in parallel with a small perturbation in initial conditions, record the separation $d(t)$, fit the slope of the linear-growth regime of $\log\ d(t)$, and average across multiple starting times to obtain $\lambda_{\text{max}}$and its uncertainty.

3. Experimental Apparatus and Data Preprocessing

3.1 Apparatus

The system is a simplified RLC magnetic rotor with a common-mode inductor. Measured signals include the pickup voltage $u_{\text{drive}}(t)$and rotor angle $\theta(t)$(radians). The rotor is driven by an AC excitation, and the sampling interval is $dt =$
0.01

3.2 Preprocessing

- Read raw data and map the angle to $[0,2\pi]$.
- Use $\sin\theta$, $\cos\theta$, and u_{drive}as input features; use θas the prediction target.
- Train/test split: the first 800 s are used for training; the remainder for testing.

LSTM

- Standardization: fit a StandardScaler on the training set and apply it consistently to both training and testing.

4. Model Construction and Experimental Procedure

4.1 Hyperparameter Selection and Training Pipeline

We select ESN hyperparameters using a combination of experience and grid search. During training, a washout period is used to discard initial transients and collect reservoir activations in the steady regime for regression. In **open-loop** prediction, the network is driven step-by-step by the standardized true test input U_{test}. In **closed-loop** prediction, after a warmup period (using the last portion of the training segment), the readout is de-standardized and fed back by converting it to $\sin(\cdot)/\cos(\cdot)$ as the angle components of the next-step input, thereby simulating autonomous evolution.

4.2 Lyapunov Estimation Details

For $\lambda_{\max}$estimation with two-trajectory divergence, we repeat experiments over N_{start}different starting points; set perturbation amplitude $\delta_0 = 10^{-6}$; use fitting window length $M_{\text{fit}} = 200$; and exclude extremely small or saturated regions to ensure the fit falls within the exponential-growth regime.

4.3 Attempt with a Low-Rank RNN

We also attempted a low-rank RNN as an alternative model to obtain a lower-rank representation of the dynamics. However, under the same training data and hyperparameter conditions, it did not yield stable pointwise prediction. Possible reasons include insufficient expressive power due to overly low rank, training instability, failure to explicitly model the driving signal, and measurement noise.

5. Results

5.1 Overview of Dynamical Behavior

By varying the driving amplitude and frequency, the system exhibits periodic, quasi-periodic, and complex (potentially chaotic) behaviors under different parameter settings.

5.2 Open-Loop Short-Term Trajectory Prediction

Under open-loop driving, the ESN demonstrates strong short-term predictive performance. The mean absolute replay error on the training segment is 0.46 rad. In the test segment, the initial short-term predictions are accurate; as time evolves, increased uncertainty leads to a slight degradation in prediction quality, and the ESN performs worse when the ground-truth signal undergoes pronounced fluctuations.

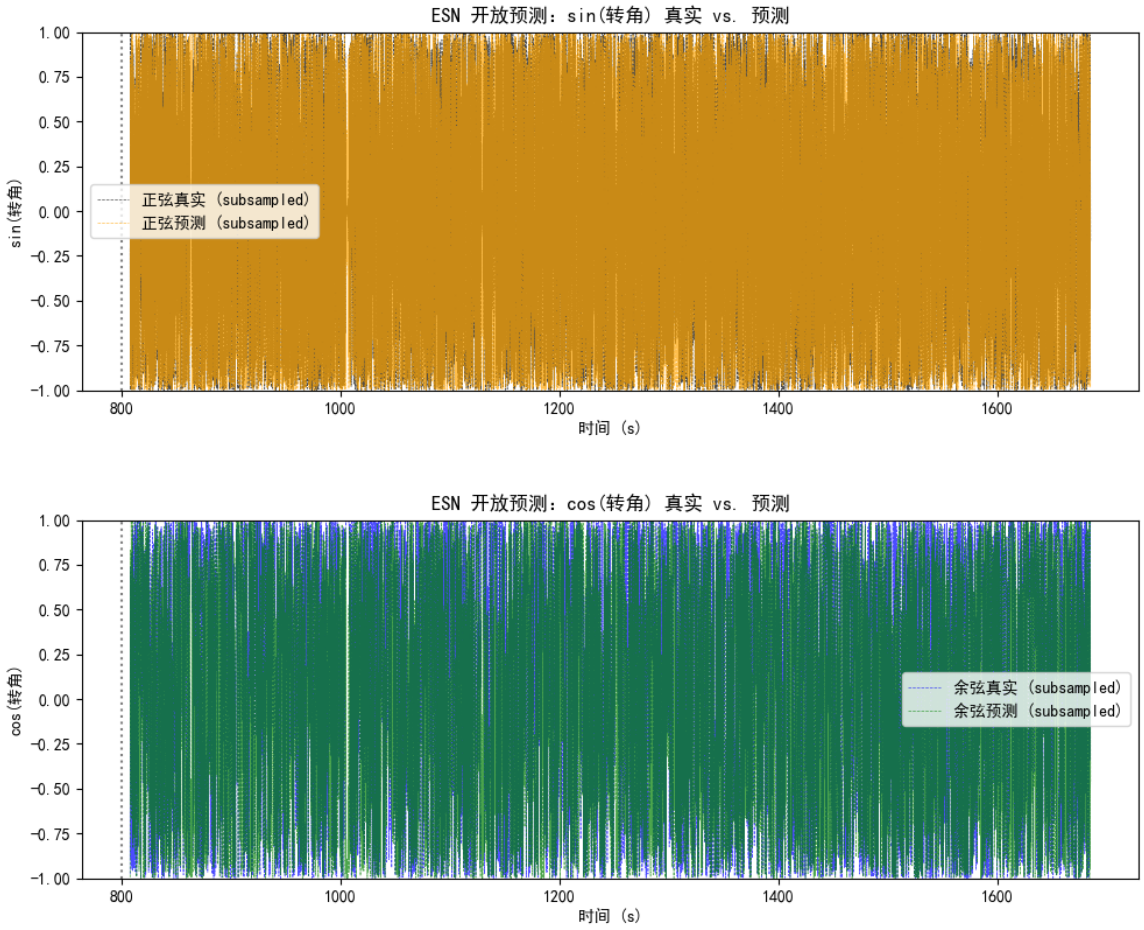

Figure 1: Training replay: true angle vs. open-loop prediction

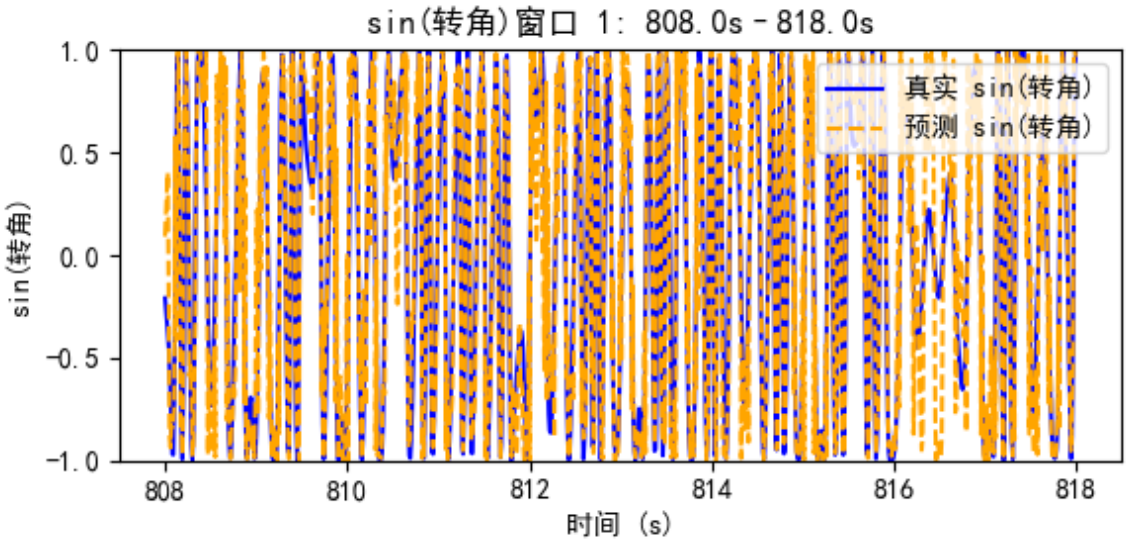
sin(转角)窗口 1: 808.0s - 818.0s
真实 sin(转角)
预测 sin(转角)
sin(转角)
时间 (s)
1.0
0.5
0.0
−0.5
−1.0
808
810
812
814
816
818

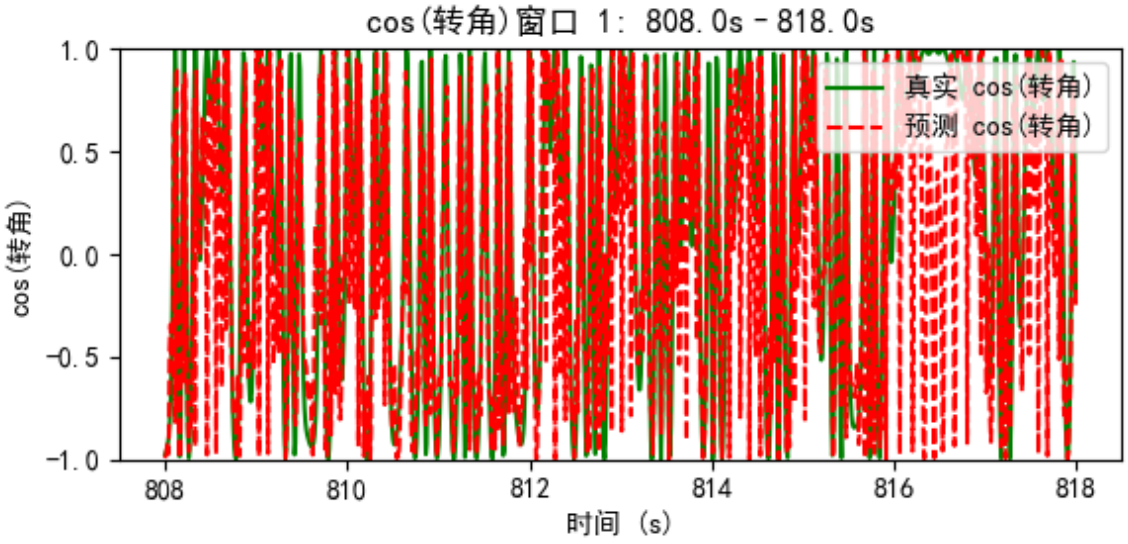
cos(转角)窗口 1: 808.0s - 818.0s
真实 cos(转角)
预测 cos(转角)
cos(转角)
时间 (s)
1.0
0.5
0.0
−0.5
−1.0
808
810
812
814
816
818

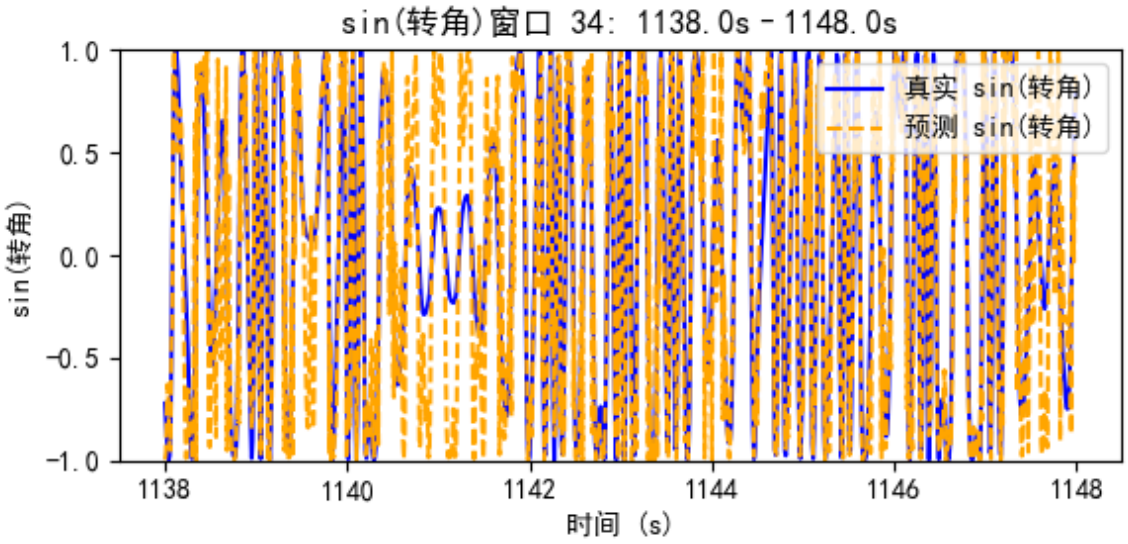
sin(转角)窗口 34: 1138.0s - 1148.0s
真实 sin(转角)
预测 sin(转角)
sin(转角)
时间 (s)
1.0
0.5
0.0
−0.5
−1.0
1138
1140
1142
1144
1146
1148

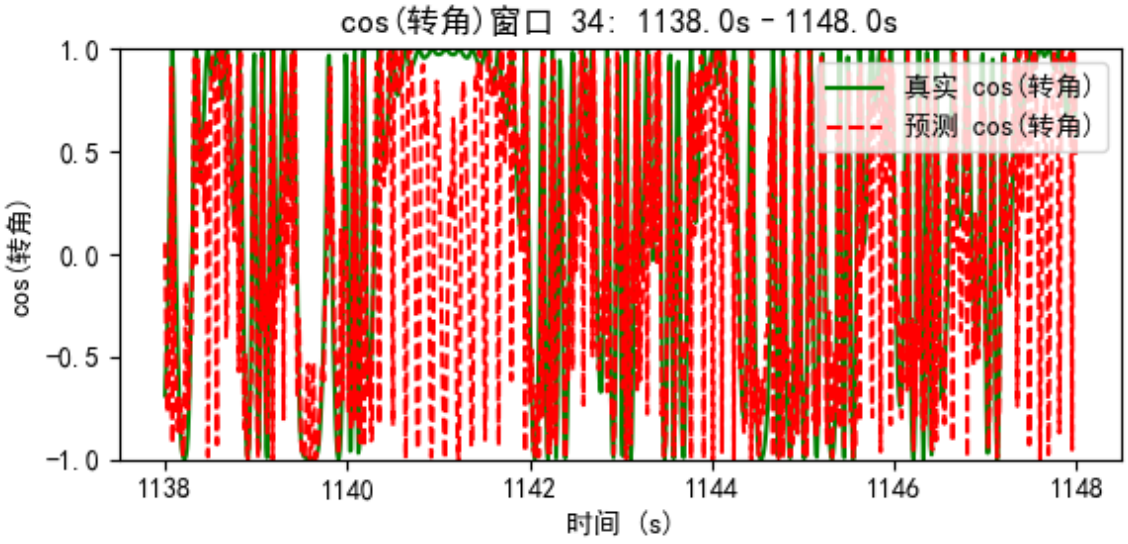
cos(转角)窗口 34: 1138.0s - 1148.0s
真实 cos(转角)
预测 cos(转角)
cos(转角)
时间 (s)
1.0
0.5
0.0
−0.5
−1.0
1138
1140
1142
1144
1146
1148

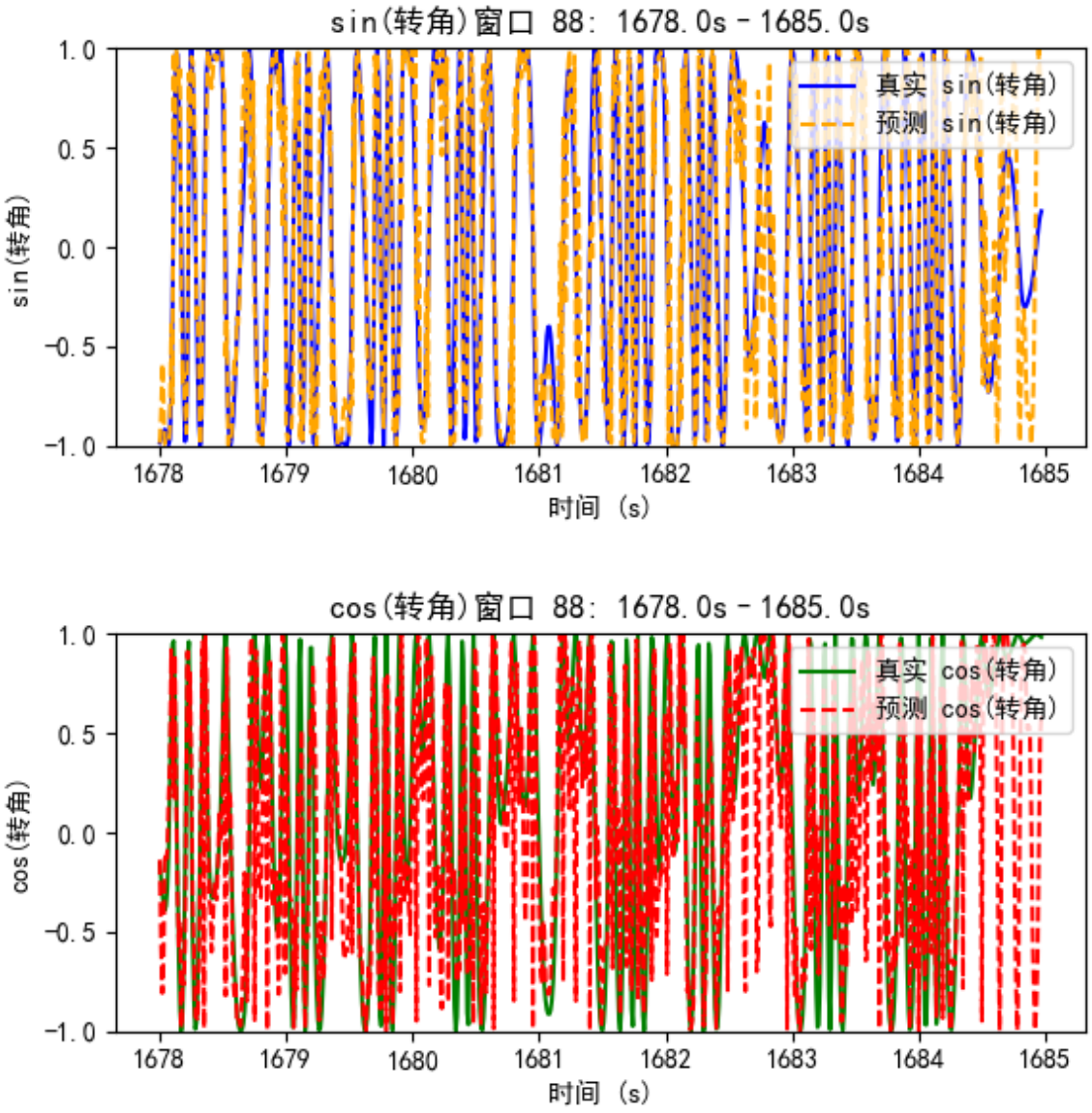

（Accuracy shows a slight decline in the later phase; however, overall predictive performance remains at a high level.）

Figure 2: Zoomed-in short-term prediction on the test set (10 s): true vs. open-loop prediction

5.3 Closed-Loop Prediction and Error Growth

After warmup, the closed-loop prediction can track the true trajectory for a short time, but the error increases over time. Over 800–1000 s, overall accuracy is lower than open-loop prediction, and the model has difficulty predicting large-amplitude variations in rotor angle.

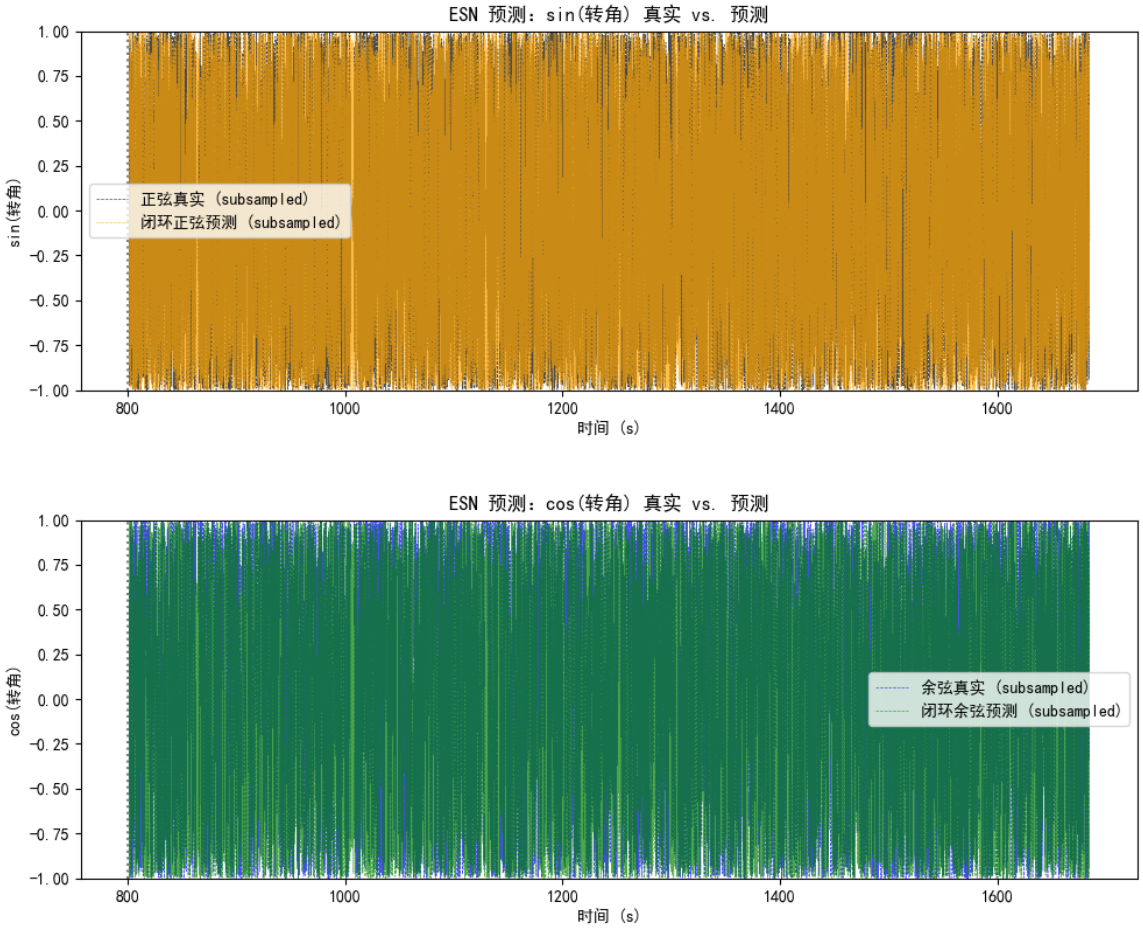

Figure 3: True angle vs. prediction (closed-loop)

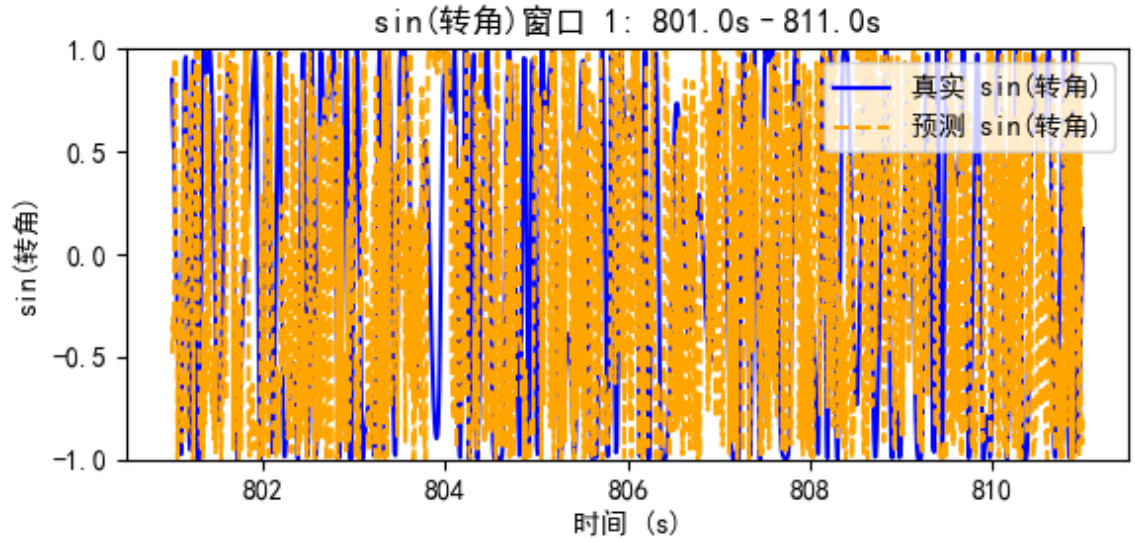

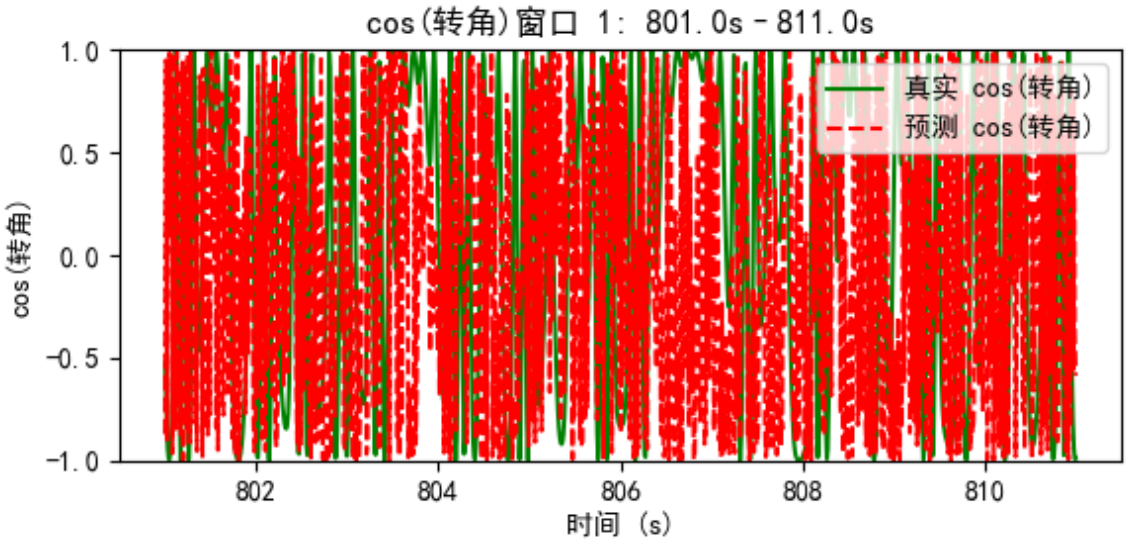
cos(转角)窗口 1: 801.0s - 811.0s
真实 cos(转角)
预测 cos(转角)
cos(转角)
时间 (s)
1.0
0.5
0.0
−0.5
−1.0
802
804
806
808
810

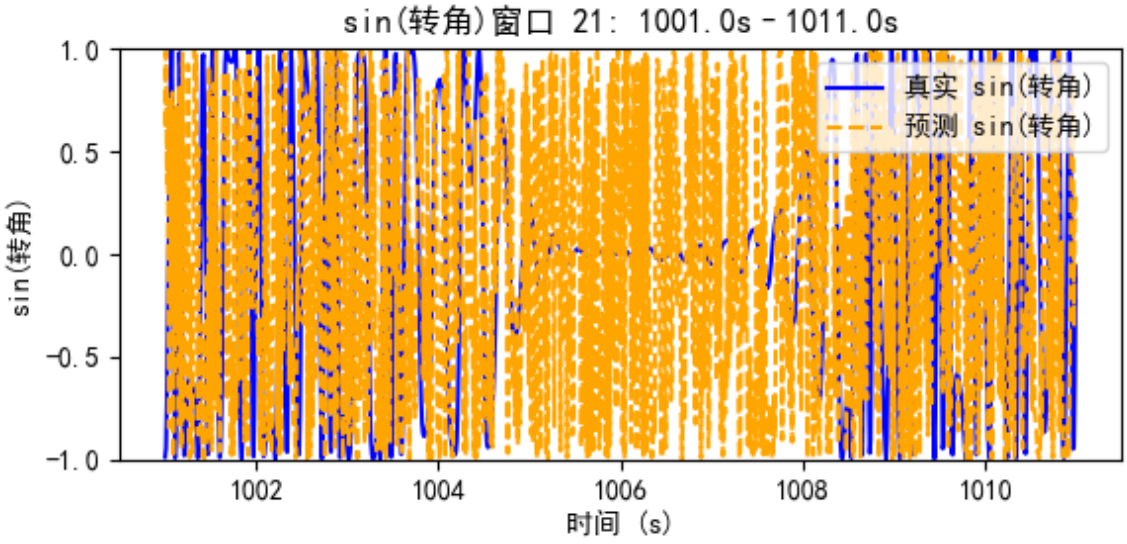
sin(转角)窗口 21: 1001.0s - 1011.0s
真实 sin(转角)
预测 sin(转角)
sin(转角)
时间 (s)
1.0
0.5
0.0
−0.5
−1.0
1002
1004
1006
1008
1010

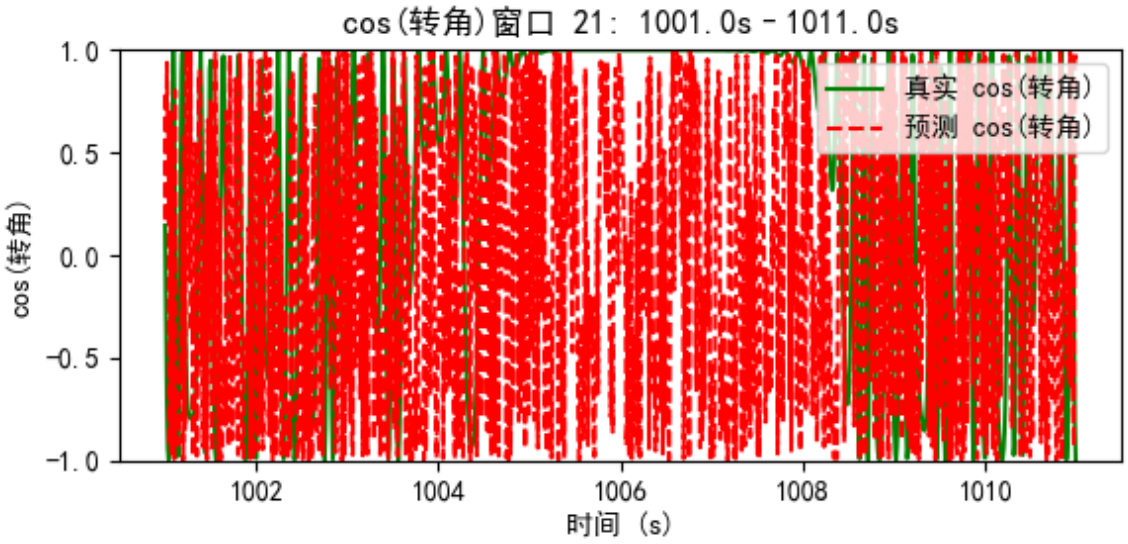

Figure 4: Zoomed-in error (samples from 800–1011 s)

5.4 Reservoir Size and Closed-Loop Performance

A grid search over reservoir sizes res_dim ∈ {390, 400, 500, 1000} reports how the 10 s closed-loop MSE varies with reservoir size. In this task, res_dim = 500 provides a practical compromise between predictive performance and computational cost.

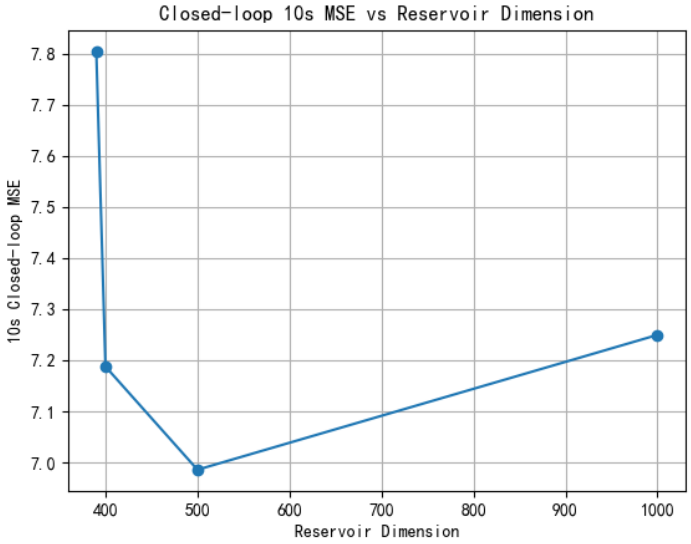

6. Discussion

6.1 Strengths and Limitations of ESNs

Strengths: fast training, high short-term prediction accuracy, and the ability to reproduce certain statistical quantities to some extent.

Limitations: in fully closed-loop mode, error grows with time and is highly sensitive to hyperparameters; robust methods are required for Lyapunov estimation, and directly fitting the true–prediction error should not be treated as a final conclusion. In the tested regime, the final closed-loop prediction yields a negative maximal Lyapunov exponent (−0.2), indicating that small perturbations decay exponentially and the system near this operating point is attractive/convergent. A negative maximal Lyapunov exponent implies weak sensitivity to initial conditions and, in principle, makes long-horizon pointwise prediction more feasible (errors would contract). In practice, however, the achievable predictability horizon is still constrained by measurement noise, model bias, and the driving signal, and the interpretation of the estimated parameter remains limited.

6.2 Diagnosing the Low-Rank RNN Failure and Suggestions

1. **Insufficient expressive power (rank too low).**
   Reason: low-rank constraints reduce the degrees of freedom in recurrent weights, limiting the ability to represent complex trajectories.
   Suggestion: test ranks in a schedule such as {2, 5, 10, 20, 50} and select the smallest rank that yields stable fitting.
2. **Train–inference mismatch / unstable optimization.**
   Reason: excessive teacher forcing, too-short BPTT windows, or learning-rate/gradient issues can cause error accumulation at inference.
   Suggestion: use scheduled sampling, Adam with learning-rate scheduling, gradient clipping (e.g., clip norm ≈ 1), and monitor gradient norms and validation loss.
3. **Measurement noise and insufficient input modeling.**
   Reason: high noise or failure to explicitly include the driving/phase as an input channel increases learning difficulty.
   Suggestion: denoise first; explicitly include the driving signal or driving phase as an input; or adopt a hybrid approach—use ESN/random reservoirs to extract high-dimensional nonlinear features, then use a low-rank RNN to model the resulting low-dimensional time series.

7. Conclusion and Future Work

1. This study demonstrates both the capabilities and limitations of ESNs for short-term trajectory prediction and statistical "climate" reconstruction in a periodically driven nonlinear experimental device. Key conclusions:

- Under open-loop driving, ESNs achieve reliable short-term prediction.
- Under closed-loop operation, pointwise predictability degrades with time, although certain statistical quantities can still be reproduced.
- Lyapunov exponent estimation must be handled with care; further statistical significance tests across more random seeds and parameter settings are needed, and hybrid schemes combining reservoir computing with low-rank RNNs are worth exploring.

2. A promising future direction is to apply autoencoder-based approaches: autoencoders can extract attractor features from experimental data in a simple and feasible manner. If a measured chaotic trajectory can be approximated as a one-dimensional manifold in latent space, one can further fit a mapping on this coordinate (e.g., a Poincaré map or a one-dimensional iterated function) and quantify complexity via symbolic dynamics. Compared with ESNs, the autoencoder–mapping approach provides a low-dimensional geometric interpretation and an interpretable dynamical model, whereas ESNs are better suited for short-term pointwise prediction and climate replication. The two approaches can be complementary—for instance, using autoencoders to extract low-dimensional features and then applying ESNs on the latent manifold, or using ESNs to generate synthetic training data to validate the mapping model. This may also offer a more intuitive and analysis-friendly path than low-rank recurrent-network methods for characterizing chaotic properties.

Advisor: Zaiqiao Bai